Dynamics of Sub-5nm Air Bearing Sliders in the Presence of Electrostatic and Intermolecular Forces at the Head Disk Interface

Vineet Gupta
Graduate Student
Dept of Mechanical Engineering
University of California, Berkeley
Email: vineet@cml.me.berkeley.edu

David B Bogy
William S. Floyd, Jr. Distinguished Professor in Engineering
Department of Mechanical Engineering
University of California, Berkeley
Email: dbogy@cml.me.berkeley.edu

Abstract

A HDI model has been used to investigate the effect of the intermolecular and electrostatic forces on the static and dynamic performance of air bearing sliders. It is seen that the intermolecular and electrostatic forces increase the level of flying height modulations at low flying heights, which in turn results in dynamic instability of the system similar to what has also been observed in experiments. In the analysis a stiffness matrix is defined to characterize the stability in the vertical, pitch and roll directions. Fly height diagrams are used to examine the multiple equilibriums that exist for low flying sliders. In addition, the simulation results are compared with previously published experiments for validation.

INTRODUCTION

AS the spacing between the slider and the disk decreases in hard disk drives, the linear bit spacing of the magnetic recording can decrease. Thus, in order to achieve an areal density of 1Tbit/in^2, the mechanical spacing between the slider and the disk has to be reduced to less than 5nm. On the other hand, due to this reduction in spacing between the slider and the disk, new forces between them come into play such as intermolecular and electrostatic forces. A study of the effect of intermolecular forces was presented in previous papers [1,2]. Here we focus on electrostatic forces in combination with the intermolecular forces. The spurious charge buildup at the head disk interface (HDI) is due to a tribocharging phenomenon. The electrostatic forces due to these charges do not have a significant effect on the flying characteristics of high flying sliders, but they become increasingly important at low head media separations. These forces are attractive in nature and hence result in a reduction in fly height as compared to what would be the case without them.

Dynamic instability has been observed experimentally for ultra low flying sliders [5]. Various HDI models have been used to explain the instability that results from the charge buildup. Some researches have studied the cause of the tribocharging phenomena at the HDI. Kiely et al. [6] developed two models, one for wear induced tribocharging and an other for surface potential induced tribocharging. They found that the overall magnitudes of both the current and the voltage are dependent on the rate of disk rotation, and using their two models they sought to predict the effect of disk rotation speed on charging. The effects of lubricants, carbon overcoats and relative humidity on tribocharging at the HDI have been studied by Feng et al [7]. They found that the tribocharging increases with the severity of head-disk interactions and decreases with conductivity of the carbon overcoat on the magnetic disk. van den Oetelaar et al. [8] also proposed two charging mechanisms. One is due to the chemical modification of the surface by the removal of oxygen bonded to the surface, and the other is due to the charge injection and trapping in electronic states in the gap of the insulating region of the diamond like carbon coating. They also studied the effect of relative humidity on tribocharging at the HDI and found that the charge buildup due to chemical modification of the surface decays at a faster rate at higher

humidity. The effect of electrostatic forces on the flying characteristics of air bearing sliders has been investigated by Song et al. [3], Knigge et al. [4], and Suk et al [5].

With the decrease in the head media spacing (in order to achieve higher areal density) the contribution of intermolecular and electrostatic forces to the force balance at the HDI can no longer be neglected. Hence it is important to investigate the dynamics of the air bearing slider under these forces. This paper is organized as follows. In the first part we present a simple 1 DOF HDI model. This simplified model is used to qualitatively study the complex nonlinear dynamics of the air bearing slider at the HDI with the aid of potential wells and phase portraits. In the second part of the paper a more complex 3 DOF air bearing model is used to study the effects of intermolecular and electrostatic forces on the stability/instability at the HDI. Further, the simulation results are compared with previously published experiments to validate our simulations.

SLIDER DYNAMICS AT THE HDI

A single DOF HDI model is first used to characterize the nonlinear dynamics of the slider under electrostatic and intermolecular forces. The differential equation that describes the fly height *z(t)* of the air bearing slider is given by

$$m\frac{d^2z}{dt^2} + c\frac{dz}{dt} + k_a(z-h) = -\nabla V_{imf}(z) - \nabla V_{elec}(z) \qquad (1)$$

where *m, c* and $k_a=\beta z^{-\alpha}$ are the effective mass (1.6 mg), the air bearing damping (0.02 Ns/m) and the nonlinear air bearing stiffness (β = 4x10^6 N/m, and α = 0.6368) respectively. The stiffness of the vertical mode is highly nonlinear for low flying sliders, so the nonlinear nature of the air bearing stiffness was considered in this analysis. The variable z describes the motion of the slider and the variable h is the steady fly height of the slider in the absence of intermolecular and electrostatic forces. $V_{imf}[z(t)]$ is the potential due to intermolecular interaction between the slider and the disk, assumed to be derived from a plane-plane interaction represented as [1,2]:

$$V_{imf}[z(t)] = -\frac{A\,dxdy}{12\pi z^2} + \frac{B\,dxdy}{360\pi z^8} \qquad (2)$$

where A (8.9238×10^{-20} J) is the effective Hamaker constant between the slider and the disk, B (10^{-76} Jm^6) is another constant and $dxdy$ (250×10^{-12} m^2) is the effective element of area on which the slider and the disk interact. $V_{elec}[z(t)]$ is the potential due to electrostatic interaction between the slider and the disk, which can be represented as:

$$V_{elec}[z(t)] = -\frac{\varepsilon_o k_e V^2 dxdy}{2z} \tag{3}$$

where ε_o, k_e and V are the permittivity constant (8.85×10^{-12} farad/m), dielectric constant of the medium (1 for air) and the potential difference between the slider and the disk.

The stability of the HDI under the influence of the electrostatic and intermolecular forces can be analyzed by considering the energy of the system. As the air bearing sliders usually have very small damping, we consider for simplicity an un-damped system. Thus the energy of the system is conserved and the potential energy method can be used to evaluate the equilibriums and analyze their stability.

The potential energy of the system which remains conserved during the motion can be expressed as:

$$U = \beta z^{-\alpha}\left(-\frac{hz}{1-\alpha} + \frac{z^2}{2-\alpha}\right) - \frac{\varepsilon_o k_e V^2 dxdy}{2z} - \frac{A\,dxdy}{12\pi z^2} + \frac{B\,dxdy}{360\pi z^8} + const \tag{4}$$

A close connection is obtained between the features of the interaction potential well and the nonlinear slider response. The criterion for an equilibrium point, z^*, is satisfied when the systems potential energy reaches a stationary point in a potential energy verses z plot. Thus the equilibrium equation reduces to

$$\frac{\partial U_{tot}}{\partial z} = 0 .$$

The equilibrium point is stable if the potential energy evaluated at the equilibrium is a local minimum, i.e.,

$$\left.\frac{\partial^2 U_{tot}}{\partial z^2}\right|_{z^*} > 0 ,$$

and it is unstable if the potential energy at the equilibrium point is a maximum, i.e.,

$$\left.\frac{\partial^2 U_{tot}}{\partial z^2}\right|_{z^*} < 0 .$$

With different initial conditions, we get slider motions corresponding to different level sets of the energy of the system. The bifurcation diagram using the simple 1-DOF model is plotted in figure 1 for the case of v = 0.5 volts. The ordinate is the equilibrium fly height between the slider and the disk in the presence of intermolecular and electrostatic forces while the abscissa is the steady state fly height between the slider and the disk in the absence of intermolecular and electrostatic forces. The potential difference between the slider and the disk is assumed to be 0.5 volts. We observe that at very low values of the numerical parameter h (say 0.6 nm) there exists one equilibrium point. For values of h between 1.36 nm and 4.81 nm, the system has three equilibrium points. And as the value of h increases beyond 4.81 nm the system has just one equilibrium point.

To analyze the stability of the various equilibrium points under the influence of the intermolecular and the electrostatic forces, we plot phase portraits and potential wells for the system. The phase portraits and potential wells as a function of the slider motion for h = 0.6, 2.0 and 5.0 nm for v = 0.5 volts are plotted in figures 2, 3 and 4 respectively.
The plot of the potential well for h = 0.6 nm shows only one stationary point and it is a local minimum. Hence this is a stable equilibrium. This can be observed in the phase portrait as well. When h is increased to 2.0 nm the potential energy curve in figure 3 shows three stationary points and hence three equilibriums. The lower and higher ones are local minima corresponding to stable equilibriums. The equilibrium point between the two stable equilibriums is a local maximum and hence it corresponds to an unstable equilibrium point. This can also be observed in the phase portrait. When h is further increased to 5.0 nm the plot of potential energy has only one stationary point and it is a local minimum. Hence this is a stable equilibrium point. This can be observed in the phase portrait as well.

The bifurcation diagram in figure 1 divides the motion of the slider into a monostable regime (far from the surface) and a bistable regime (close to the surface) where two stable and one unstable equilibriums coexists. Here the equilibrium closer to the surface has a head media separation less than 0.3 nm. Thus it corresponds to a state where the slider is effectively stuck to the disk surface. The 1-DOF model was used to understand the dynamics of the HDI qualitatively. For quantitative analysis we next consider a 3-DOF model.

3 DOF HEAD DISK INTERFACE MODEL

When an air bearing slider is flying at sufficiently low mechanical separations the significant forces acting on it are the suspension force, air bearing force, contact force, shear force, intermolecular force and the electrostatic force. To calculate the static flying characteristics of the air bearing slider, we consider a 3 DOF model in the variables fly height (z), pitch (θ) and roll (φ). The following force and moment balance equations are used to model the dynamics of the slider.

$$m\frac{d^2z}{dt^2} = F_{su} + F_c + F_{imf} + F_{elec} + \int (p - p_a)dA \tag{5}$$

$$I_\theta \frac{d^2\theta}{dt^2} = M_{su\theta} + M_{sh\theta} + M_{c\theta} + M_{imf\theta} + M_{elec\theta} + \int (p - p_a)(x_g - x)dA \tag{6}$$

$$I\varphi \frac{d^2\varphi}{dt^2} = M_{su\varphi} + M_{sh\varphi} + M_{c\varphi} + M_{imf\varphi} + M_{elec\varphi} + \int (p - p_a)(y_g - y)dA \tag{7}$$

where,

$$F_{elec} = -\frac{\varepsilon_o k_e V^2}{2} \iint_{area} \frac{dxdy}{z^2}, \text{ and} \tag{8}$$

$$F_{imf} = -\frac{A}{6\pi} \iint_{area} \frac{dxdy}{z^3} + \frac{B}{45\pi} \iint_{area} \frac{dxdy}{z^9} \tag{9}$$

The relationship between the pressure distribution (P) and the HDI spacing (z) is given by the non-dimensional generalized Reynolds equation.

$$\frac{\partial}{\partial X}\left(QPH^3 \frac{\partial P}{\partial X} - \Lambda_x PH \right) + \frac{\partial}{\partial Y}\left(QPH^3 \frac{\partial P}{\partial Y} - \Lambda_y PH \right) = \sigma \frac{\partial}{\partial t}(PH) \tag{10}$$

These equations are used to calculate the dynamic response of the air bearing slider. The Quassi-Newton iteration method is implemented to calculate the static solutions, the case where all the time dependent terms vanish.

In order to have a stable HDI, the total stiffness in the vertical, pitch and roll directions must be positive. In other words the total bearing load capacity must be positive. It has been found that at ultra low fly heights the z-stiffness value decreases as the fly height decreases, and it becomes negative below a critical fly height value. Negative stiffness means that the bearing is unable to maintain a mechanical spacing between the slider and the disk, which leads to contact.

The matrix equation relating changes in the forces in the z direction and moments in the pitch and roll directions to the changes in the fly height (z), pitch (θ) and roll (φ) can be mathematically represented as

$$\begin{bmatrix} dF \\ dT_\theta \\ dT_\varphi \end{bmatrix} = \begin{bmatrix} \frac{\partial F}{\partial z} & \frac{\partial F}{\partial \theta} & \frac{\partial F}{\partial \varphi} \\ \frac{\partial T_\theta}{\partial z} & \frac{\partial T_\theta}{\partial \theta} & \frac{\partial T_\theta}{\partial \varphi} \\ \frac{\partial T_\varphi}{\partial z} & \frac{\partial T_\varphi}{\partial \theta} & \frac{\partial T_\varphi}{\partial \varphi} \end{bmatrix} \begin{bmatrix} dz \\ d\theta \\ d\varphi \end{bmatrix} \tag{11}$$

This 3x3 matrix of first derivatives is called the stiffness matrix.

The system is stable only if it is stable in all three directions, i.e. z, pitch and roll. Mathematically, if all three eigenvalues of the stiffness matrix are positive, then the system is stable. But if one or more of the eigenvalues of the stiffness matrix are negative, then the system is unstable.

In this study the stability/instability of the HDI is analyzed using a "fly height diagram". The fly height diagram plots the slider fly height versus disk rpm. The minimum mechanical spacing between the slider and the disk is referred to as the fly height. A typical fly height diagram is shown in figure 5. The points on curve 1 give the steady state fly height as a function of disk rpm without considering the effects of intermolecular and electrostatic forces. All of the points on this curve have positive stiffness values and hence represent stable conditions. Curves 2 and 3 plot the fly height versus disk rpm taking into consideration the effect of intermolecular and electrostatic forces. From the figure we observe multiple equilibrium points for disk rpms between 1900 and 4300. The equilibrium points on curve 2 have positive stiffness values and hence are stable equilibrium points. However the points on curve 3 have negative stiffness values and hence are unstable equilibrium points.

From the fly height diagram we observe that as the disk rpm decreases from 12000 to as low as 1900, a stable fly height is given by the curve 2. Below 1900 rpm (corresponding to a fly height of 3.4nm) the slider becomes unstable and contact occurs between the slider and the disk. This value of disk rpm gives the touchdown rpm. If the disk rpm is increased from 1900, the slider remains unstable until a disk rpm of 4300. For

rpm's above 4300 (corresponding to a fly height of 5.05nm) there is only one equilibrium point, which is stable and hence the stability of the HDI is restored at 4300. This value of rpm gives the takeoff rpm. The rpm range of curve 3 in the fly height diagram gives an estimate of the hysterisis observed in touchdown-takeoff experiments. We can also conclude that the larger the range of the unstable region (curve 3), the higher will be the hysterisis observed in the touchdown-takeoff experiments. A detailed description of the fly height diagram is given in references [1,2].

Static simulations were carried out for the slider design shown in figure 6 for potential differences of V = 0.3 volts and V= 1.0 volts, with and without intermolecular forces. The fly height diagrams are shown in figure 7. The equilibrium points for which the head media spacing is less than 0.3 nm are considered to be contact and are not included in this fly height diagram.

We found that the hysteretic behavior depends on the potential difference between the slider and the disk, which characterizes the strength of the interaction. The potential difference between the slider and the disk increases the width of the unstable region regardless of whether the intermolecular forces are present. On comparing the fly height diagrams for the cases with V = 0.0 volts and V = 0.3 volts, we observe that a potential difference of 0.3 volts does not have a significant effect for fly heights greater than 4 nm. But on the other hand a potential difference of 1 volt has a very significant effect even at higher fly heights.

To validate our simulation results we carried out static simulations for the slider design shown in figure 6 with intermolecular forces and various values of V. A suitable disk rpm was chosen at which the slider's fly height was 30 nm with V = 0 volts. The potential difference was then increased between the slider and the disk until the air bearing was unable to maintain the spacing between the slider and the disk, i.e. the stiffness becomes negative and contact occurs as shown in figure 8.

These results are compared with similar experimental results recently published by Song et al [3]. Excellent agreement is seen between the simulation results and the experimental data. Similar simulations were also carried out for two other 30 nm fly height slider designs. We found that the simulation results were not exactly the same as shown in figure 8, but the differences were not much.

Static simulations were also carried out at suitable disk rpm's such that the slider design shown in figure 6 has fly height's of 15nm, 10nm and 5nm for V = 0 volts. The breakdown voltages were then calculated for these three cases. Figure 9 shows the increase in breakdown voltage as the slider fly height increases. As expected for high flying sliders the air bearing can withstand higher voltage across it before it breaks down.

But on the other hand as the potential difference between the slider and the disk increases the air bearing breaks down at higher fly heights. For example, for a 30 nm flying slider, when the potential difference between the slider and the disk increases the fly height decreases and the air bearing finally breaks down at a spacing of 9.45 nm when the potential difference is 7.13 volts, and for a 15 nm flying slider the air bearing breaks down at 4.65 nm when the potential difference between the slider and the disk in 3.96 volts.

Further, static simulations were carried out for the two different slider designs shown in figures 6 and 10. Suitable disk rpm's were chosen for both slider designs so that they fly at 5 nm. The slider design shown in figure 6 is a higher pitch slider with a pitch angle close to 245 μrad and the slider design shown in figure 10 is a lower pitch slider with a pitch angle close to 190 μrad.

The potential difference was then increased between the slider and the disk in the simulations until the air bearing was unable to maintain the spacing between the slider and the disk, i.e. the stiffness becomes negative and contact occurs as shown in figure 11. We observe that the high pitch slider air bearing can sustain higher voltage across it before it breaks down. It was also observed that as the potential difference between the slider and the disk increases the magnitude of the pitch angle also increases slightly.

The dynamic response was also simulated at a disk rpm of 7200 for the slider design shown in figure 6. The slider is "dropped" from a 10 nm fly height. We observe that the solver converges to a steady state when the potential difference between the slider and the disk is 0.3 volts and 1.0 volts as shown in the figure 12. But for higher potential differences the system becomes unstable and contact occurs between the slider and the disk. From the fly height diagram shown in figure 7 we observe that at the disk rpm of 7200 there exists only one (stable) equilibrium point when the potential difference

between the slider and the disk is 0, 0.3 and 1.0 volts. Hence the system always converges to a steady state for small perturbations about the equilibrium point as shown in figure 12.

CONCLUSION

A HDI model was developed to investigate the effect of intermolecular and electrostatic forces on the static and dynamic performance of air bearing sliders. Static simulations were carried out for various values of potential difference between the slider and the disk. It was found that the electrostatic forces due to charge buildup are attractive in nature and hence reduce the fly height as has been observed experimentally. This phenomenon becomes increasingly important at low head media separations. A slight increase in the magnitude of the pitch angle is also observed as the potential difference between the slider and the disk increases.

We also presented a theoretical investigation of the stability and dynamics of air bearing sliders at the head disk interface. Further, a stability criteria based on the potential energy was derived that helped to better explain the instabilities that appear at the HDI when the slider is flying very close to the disk surface. The motion of the slider was divided into two regimes -- a monostable regime, far from the surface and a bistable regime, close to the surface where the two stable and one unstable equilibriums coexists. A 1-DOF model was used to understand the dynamics of the HDI qualitatively. For quantitative analysis we considered a 3-DOF model. A fly height diagram is used to analyze the stability of the HDI. It is observed that high flying sliders can withstand higher potential difference between the slider and the disk before the air bearing breaks down. We also found that high pitch sliders are more stable in the presence of intermolecular and electrostatic forces. Further, the simulation results were compared with previously published experiments giving strong validation of the 3-DOF model.

REFERENCES

[1.] V. Gupta, and D.B. Bogy, "Effect of Intermolecular Forces on the Static and Dynamic Performance of Air Bearing Sliders: Part I – Effect of initial excitation and slider form factor on the stability," *ASME Journal of Tribology* (accepted for publication).

[2.] V. Gupta, and D.B. Bogy, "Effect of Intermolecular Forces on the Static and Dynamic Performance of Air Bearing Sliders: Part II – Dependence of the stability on the Hamaker constant, suspension preload and pitch angle," *ASME Journal of Tribology* (accepted for publication).

[3.] D. Song, D. Schnur and Z. Boutaghou, "Mechanism of Discharge At The Head Disk Interface," no CC-07, *9th InterMAG conference*, 2004.

[4.] B. Knigge, C. Mate, O. Ruiz, and P.M. Baumgart, "Influence of Contact Potential on Slider-Disk Spacing: Simulation and Experiment," no CC-08, *9th InterMAG conference*, 2004.

[5.] M. Suk, R. Kroeker, and D. Gills, "Investigation of slider dynamics under electro-static force," *Microsystem Technologies*, vol 9, no 4, pp. 256-265, 2003.

[6.] J.D. Kiely, and Y.T. Hsia, "Tribocharging of the magnetic hard disk drive head-disk interface," *Journal of Applied Physics*, vol 91, no 7, pp. 4631-4636, Apr 2002.

[7.] Zhu Feng, Chug Shih, Vidya Gubbi and Frank Poon, "A study of tribo-charge/emission at the head-disk interface," *Journal of Applied Physics*, vol 85, no 8, pp. 5615-5617, Apr 1999.

[8.] R.J.A. van den Oetelaar, L. Xu, D.F. Ogletree, M. Salmeron, H. Tang and J. Gui, "Tribocharging phenomena in hard disk amorphous carbon coating with and without perfluoropolyether lubricants," *Journal of Applied Physics*, vol 89, no 7, pp. 3993-3998, Apr 2001.

[9.] A.J. Wallash, "Electrostatic Discharge and Electrical Breakdown Study of the Head-Disk Interface in a Hard Disk Drive," *IEEE Transactions on Magnetics*, vol 40, no 3, may 2004.

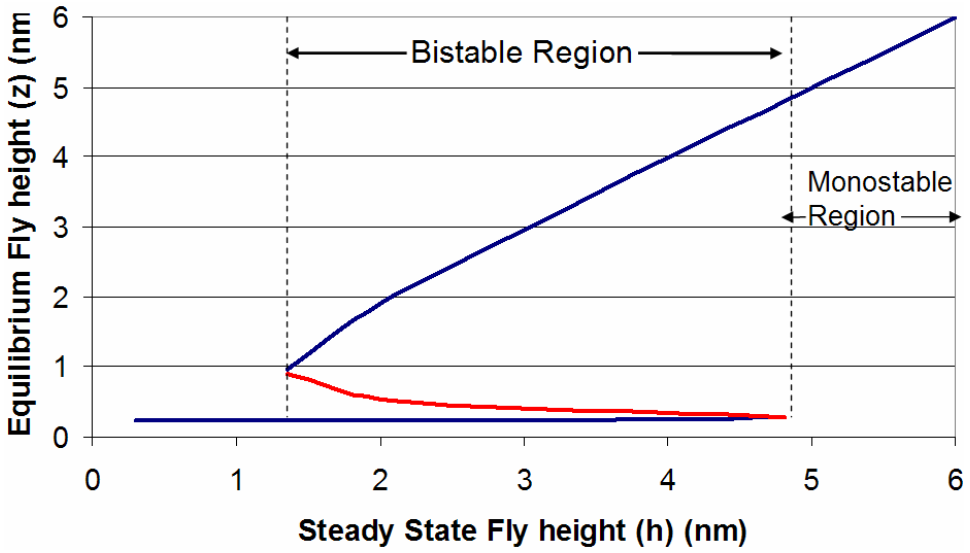

Fig. 1. Bifurcation diagram using 1 DOF model for V = 0.5 volts with both intermolecular and electrostatic forces included. We observe bistable and monostable regions.

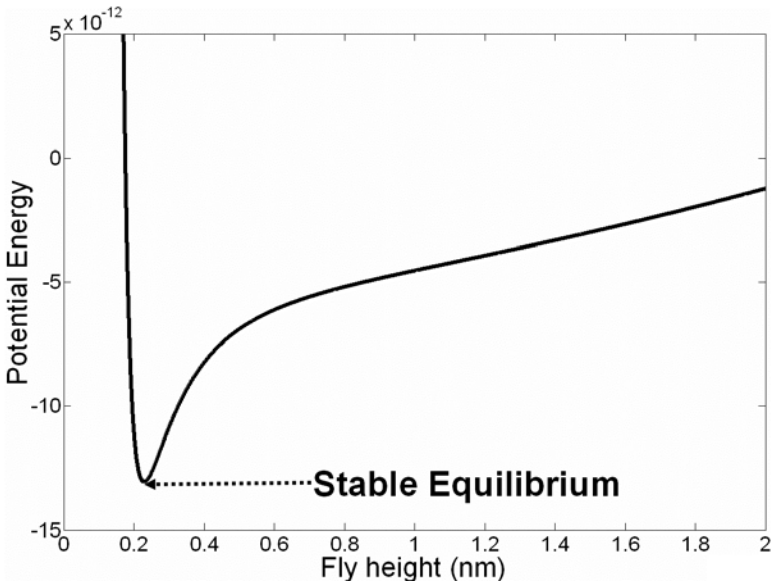

(a)

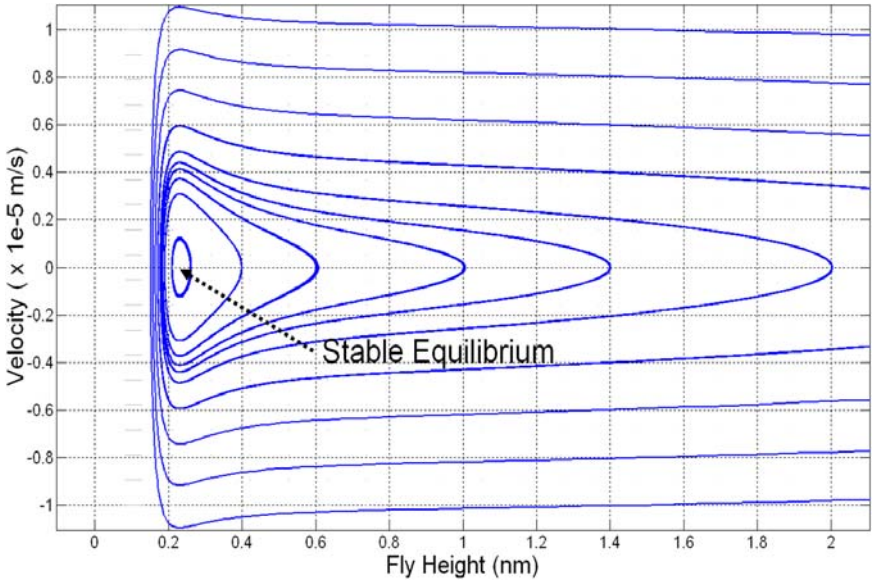

(b)

Fig. 2. (a) Potential energy curve and (b) phase portrait for h = 0.6 nm

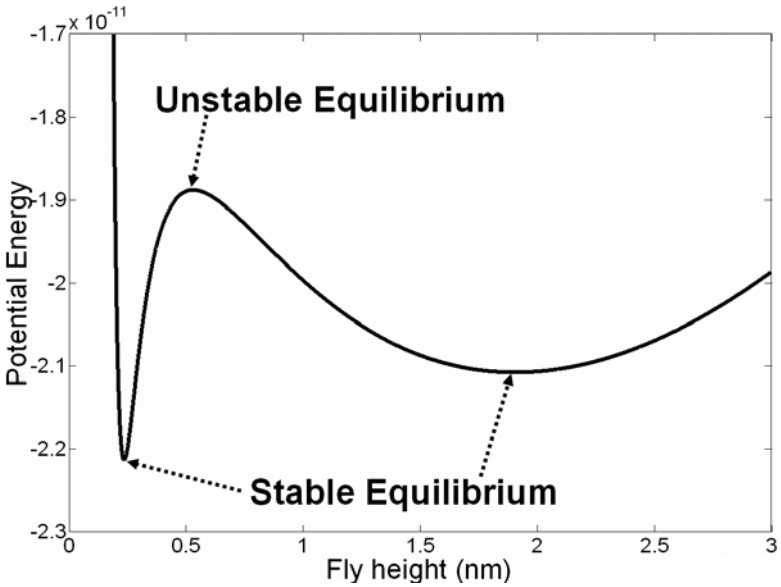

(a)

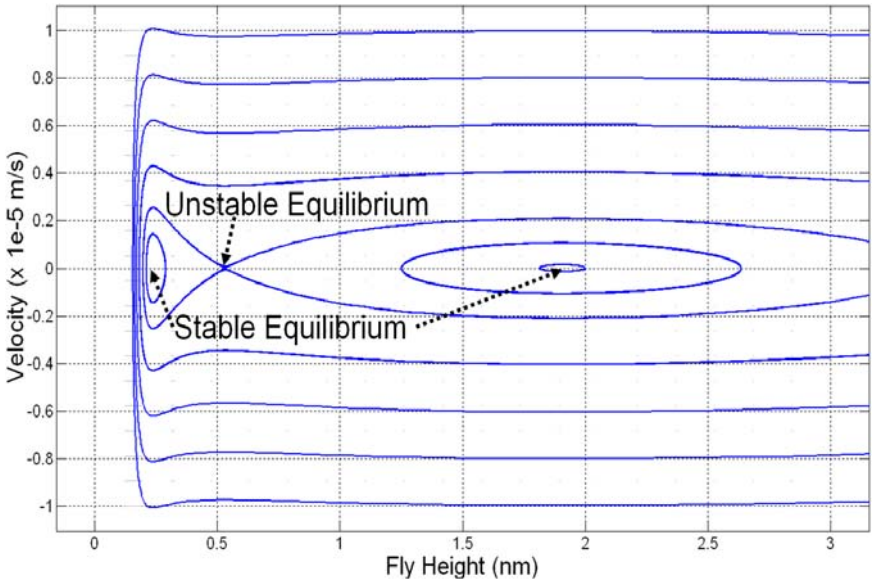

(b)

Fig. 3. (a) Potential energy curve and (b) phase portrait for h = 2 nm

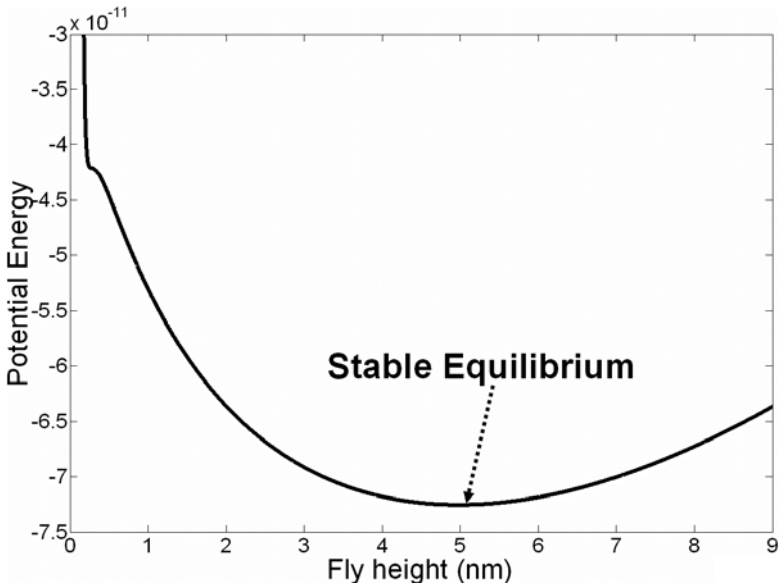

(a)

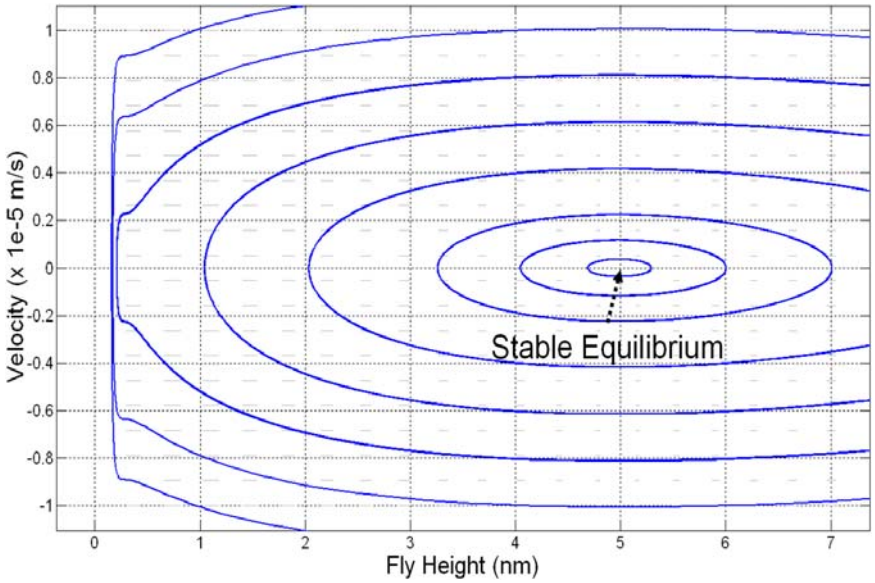

(b)

Fig. 4. (a) Potential energy curve and (b) phase portrait for h = 5 nm

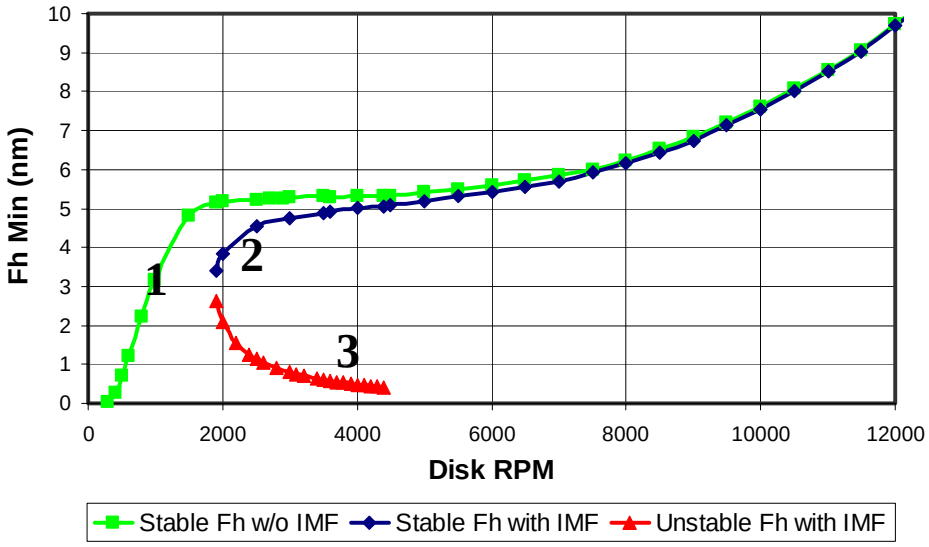

Fig. 5. Fly height (Fh) diagram

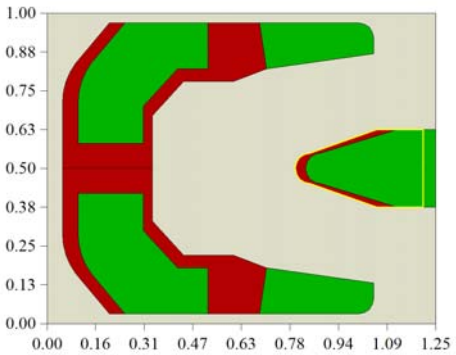

Fig. 6. High pitch pico slider with crown of 30 nm and a camber of -5 nm. The base recess is 1.397 μm.

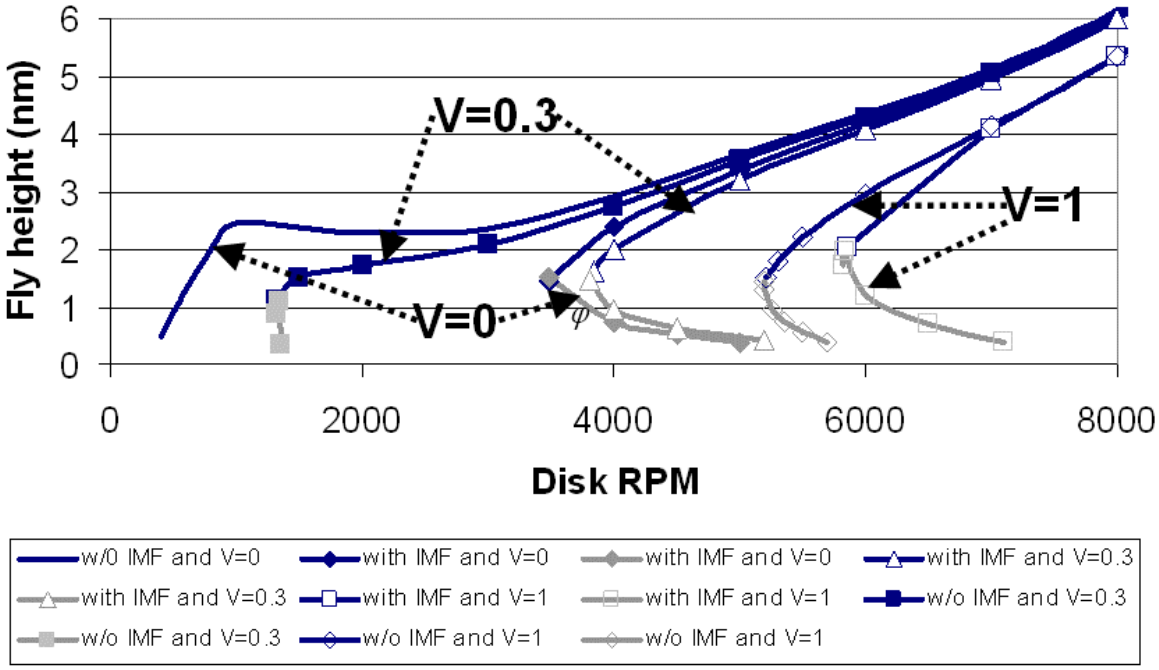

Fig. 7. Fly height Diagram using 3 DOF HDI model for slider design shown in fig. 6

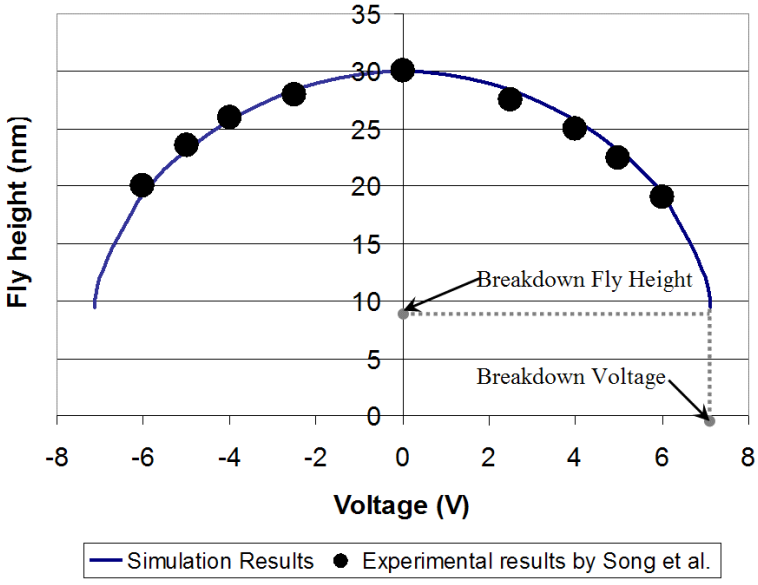

Fig. 8. Fly height variation as a function of potential difference

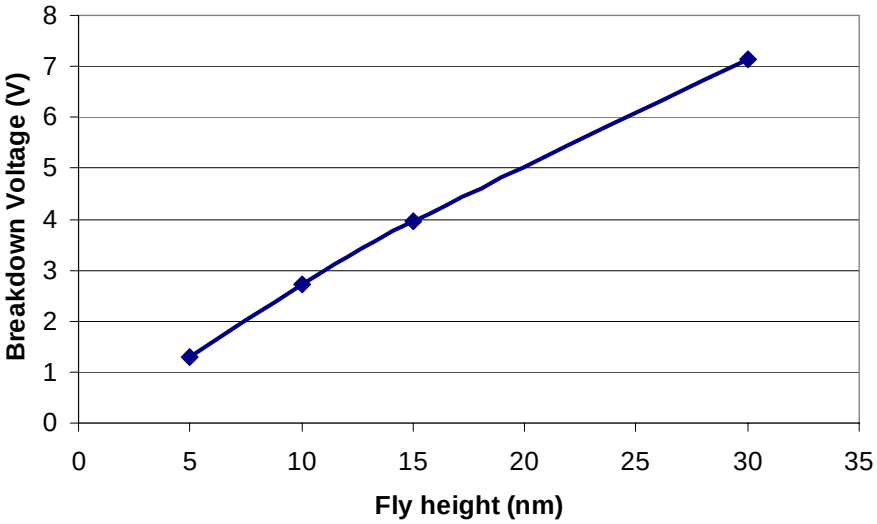

Fig. 9. Increase in breakdown potential as the slider fly height increases.

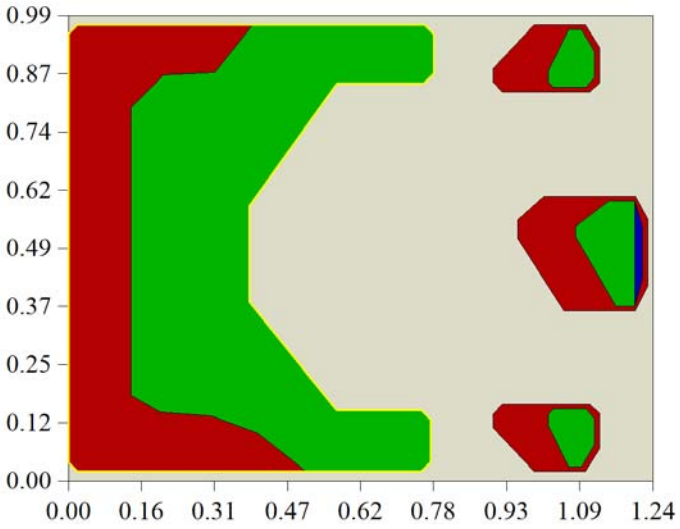

Fig. 10. Low pitch pico slider with crown of 30 nm and a camber of -5 nm. The base recess is 1.397 μm.

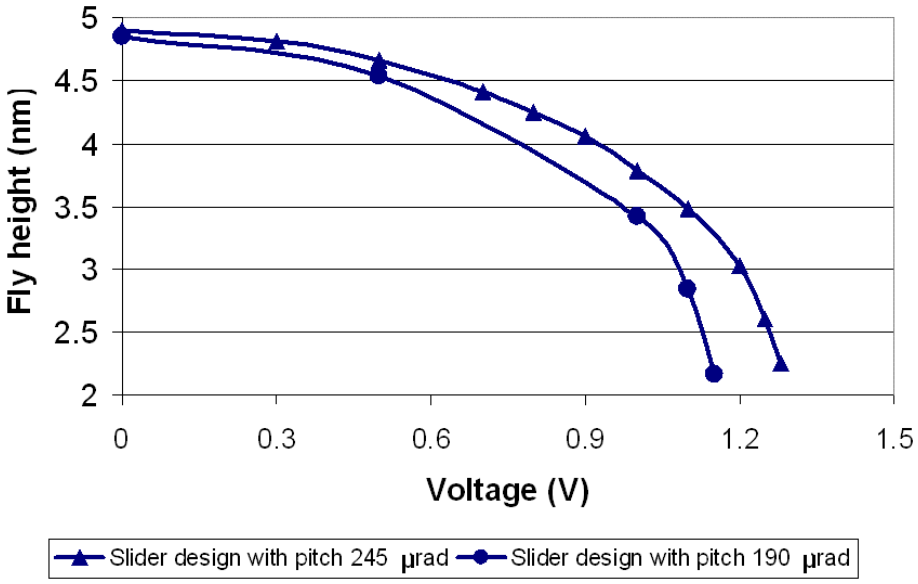

Fig. 11. Fly height variation as a function of potential difference.

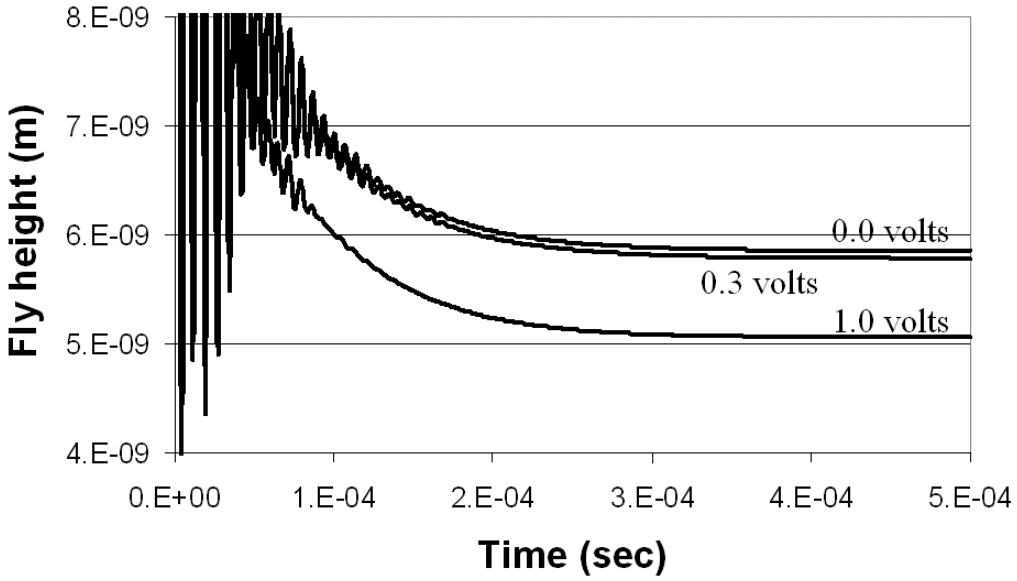

Fig. 12. Dynamic response of the slider in figure 6 at a disk rpm of 7200 as the potential difference increases between the slider and the disk.